

# Force Characterization of a Rotary Motion Electrostatic Actuator based on Finite Element Method (FEM) Analysis

MD GHAZALY Mariam<sup>1,a</sup>, TAN Aik Choon<sup>1</sup>, CHE AMRAN Aliza<sup>1</sup> and SATO Kaiji<sup>2</sup>

<sup>1</sup>Center for Robotic and Industrial Automation (CeRIA), Faculty of Electrical Engineering, Universiti Teknikal Malaysia Melaka, Hang Tuah Jaya, 76100 Durian Tunggal, Melaka, Malaysia

<sup>2</sup>Interdisciplinary Graduate School of Science and Engineering, Tokyo Institute of Technology, 4259-G2-17 Nagatsuta Midori-ku, Yokohama 226-8502, Japan

[amariam@utem.edu.my](mailto:amariam@utem.edu.my)

**Keywords:** Rotary Motion, Rotary Actuator, Electrostatic Actuator, Actuation Thrust Force, FEM Analysis.

**Abstract.** Two types of rotary motion electrostatic actuators were designed and analyzed using Finite Element Method (FEM) analysis. This paper discussed the comparisons and detailed thrust force analysis of the two actuators. Both designs have similar specifications; i.e the number of rotor's teeth to stator's teeth ratio, radius and thickness of rotor, and gap between stator and rotor. Two structures were designed & evaluated; (a) Side-Driven Electrostatic Actuator and (b) Bottom-Driven Electrostatic Actuator. The paper focuses on comparing & analyzing the generated electrostatic thrust force for both designs when the electrostatic actuator's parameters are varied. Ansys Maxwell 3D software is used to design and analyze the generated thrust force of the two rotary motion electrostatic actuators. The FEM analyses have been carried out by (i) varying the actuator size; (ii), varying the actuator thickness and (iii) varying the actuator teeth ratio. The FEM analysis shows that the Bottom-Drive Electrostatic Actuator exhibit greater thrust force, 4931.80 $\mu$ N compared to the Side-Drive Electrostatic Actuator, 240.96 $\mu$ N; when the actuator's radius is 700 $\mu$ m, thickness is 50 $\mu$ m, gap between the stator and rotor is 2 $\mu$ m and the teeth ratio is 16:12.

## Introduction

Nowadays, the growth of interest in Micro Electro Mechanical System (MEMS) is increasing rapidly. MEMS consists of micromechanisms such as microstructures, microactuators and microsensors. Microactuator is a subset of microelectromechanical systems (MEMS) that convert electrical energy to mechanical energy. With advance technologies in microfabrication for MEMS, an efficient and reliable microactuator can be built for various microsystems. Microactuators can be used for development in biotechnology, medicine, communication and inertial sensing. Several types of microactuators have been studied widely such as the electrostatic microactuator, piezoelectric microactuator and electromagnetic microactuator [1,2]. Table 1 shows the comparison of the general characteristics of the microactuators, which consist of two motion drives, i.e (i) linear motion and (ii) rotary motion. From Table 1, the rotary actuator able to apply to a large working range compared to the linear actuator. In comparison, both electrostatic and electromagnetic actuator able to generate a better thrust force compared to the piezoelectric actuator. Although electromagnetic actuators are the most widely used, electrostatic actuators have some advantages in terms of their heat production and material availability compared with electromagnetic actuators [3]. In addition, unlike piezoelectric actuators, electrostatic actuators are able to transmit power without mechanical contact and do not require hinges, which make the systems complex. Previously, various types of electrostatic actuators have been designed which show good performances.

As a solution, in this paper two types of rotary type electrostatic actuator are designed in order to evaluate the generated thrust force. For the electrostatic actuator, the size, actuator rotor ratio and the applied voltage will effect the generated thrust force. The aim of this paper is to optimum the actuators parameters that would generate the best actuation force based on two different rotary actuator design.

Table 1 General characteristics of microactuators

Microactuators	Motion Type	Working Range	Thrust Force
Electrostatic	Linear	Small	High
	Rotary	Large	Medium to high
Piezoelectric	Linear	Small	High
	Rotary	Large	Low to medium
Electromagnetic	Linear	Small to medium	High
	Rotary	Large	Medium to high

### Rotary Motion Electrostatic Microactuator

#### Actuation Principle

A rotary motion microactuator in general consists of a rotor and a stator, both having several number of teeth-like electrodes. During operation, the rotor electrodes are grounded and the stator electrodes are grouped in three different electrical phases that are symmetrically distributed around the rotor. Each phase can be activated independently. At the initial position, the electrodes of the first phase are perfectly aligned with the opposite electrodes of the rotor side. By applying voltage differences on one of the misaligned phases, electrostatic thrust force can be generated. Clockwise or counter-clockwise stepwise motion can be achieved by changing the phase sequences [3].

#### Design Structures: Side-Driven and Bottom-Driven

Fig. 1 shows the three-dimensional view of two designs; (a) Side-Driven Electrostatic Microactuator and (b) Bottom-Driven Electrostatic Microactuator which comprise of 12 stators and 16 poles rotor [4]. The rotor of the Side-Driven is mounted inside the stator. However for the Bottom-Driven, the stator is mounted directly above the rotor, which increases the thickness of the actuator. Both designs function as a three-phase microactuator. The diameter of rotor is 1.4mm and the gap between the stator and rotor is  $2\mu\text{m}$  for both designs. The initial dimensions of the two designs are listed in Table 2. The operation of these microactuators relies on the electrical energy stored in the variable capacitances formed between the poles of the rotor and the stator. The stator poles are connected in an alternative sequence with three electrical phases; each phase activates a group of stator independently. When a phase is activated, a voltage difference between the corresponding stator poles and the opposite rotor poles generates an electrostatic force which realign the poles of rotor with the activated stator poles.

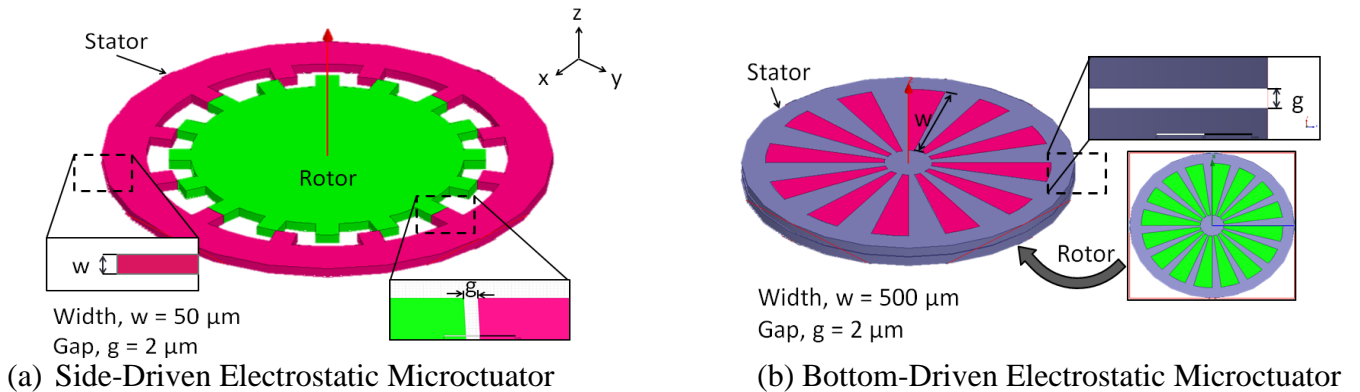


Fig. 1 Two design of the rotary motion electrostatic microactuator

## Force Characteristics and Design Optimization using FEM Analysis

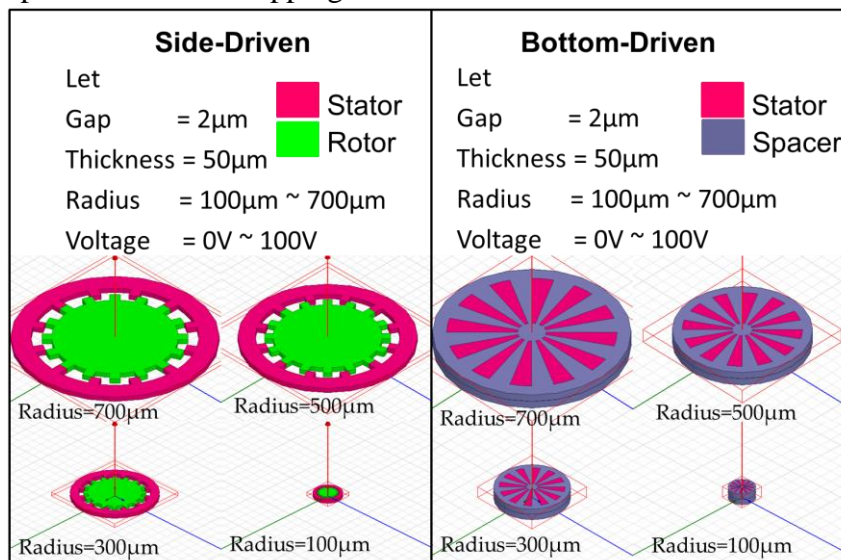
In order to optimize the design parameter's of the rotary electrostatic microactuator, ANSYS Maxwell 3D was used to analyse the electrostatic thrust force of both designs. Simulations are done by varying the actuator's parameters using Finite Element Method (FEM) analysis. The paramnters varied are (i) actuator size; (ii) actuator thickness and (iii) actuator teeth ratio.

Table 2 Initial design parameters

Parameter	Symbol	Value
Rotor radius	$r$	700 $\mu\text{m}$
Pole width (Side-Driven)	$w_1$	50 $\mu\text{m}$
Pole width (Bottom-Driven)	$w_2$	500 $\mu\text{m}$
Gap (rotor/stator)	$d$	2 $\mu\text{m}$
No. of active poles per phase	$n$	4

### Varying Actuator Size

The size of both actuators were set to seven values; i.e 100 $\mu\text{m}$  to 700 $\mu\text{m}$  respectively, whilst the gap between the stator and the rotor, teeth ratio and thickness of actuator is fixed to 2 $\mu\text{m}$ , 16:12 and 50 $\mu\text{m}$ , respectively. The FEM analysis was implemented by applying input voltage to the actuator. Fig. 2 shows both the structures of the Side-Driven and Bottom-Driven with different sizes. Fig. 3 shows the relationship between the size of actuator, applied voltage and the generated electrostatic force. From Fig. 3, it can be depicted that, as the size of actuators decreases, the overlapping area between the rotor and the stator electrodes will also decreased, which results in lower thrust force. By comparing Fig. 3 (a) and (b), the electrostatic force of Bottom-Driven Electrostatic Microactuator is higher than the electrostatic force of Side-Driven Electrostatic Microactuator because of the area overlapping of Bottom-Driven actuator is larger than area overlapping of Side-Driven actuator. Therefore, it can be concluded that electrostatic force depends on the overlapping area between the stator and the rotor electrodes.



(a) Side-Driven Electrostatic Microactuator (b) Bottom-Driven Electrostatic Microactuator

Fig. 2: Structure comparison between the side-driven and bottom-driven microactuator, when the size is varied.

### Varying Actuator Thickness

The thickness of both actuators were set to five values; i.e 10 $\mu\text{m}$  to 50 $\mu\text{m}$  respectively, whilst the gap between the stator and the rotor, teeth ratio and size of actuator is fixed to 2 $\mu\text{m}$ , 16:12 and 700 $\mu\text{m}$ , respectively. Fig. 4 shows the relationship between the thickness of actuator, applied voltage and the generated electrostatic force. From Fig. 4, changing the thickness of side-drive actuator does affect the

electrostatic force produced because the area overlapping depends the actuator's thickness. However, it can be depicted that changing the thickness of bottom-drive actuator does not affect the electrostatic force because the area overlapping of bottom-drive actuator does not depend on the thickness of actuator. By comparison, the Bottom-Driven actuator produced greater electrostatic force than Side-Driven actuator although manipulating the thickness of actuator does not significantly affect the generated electrostatic force.

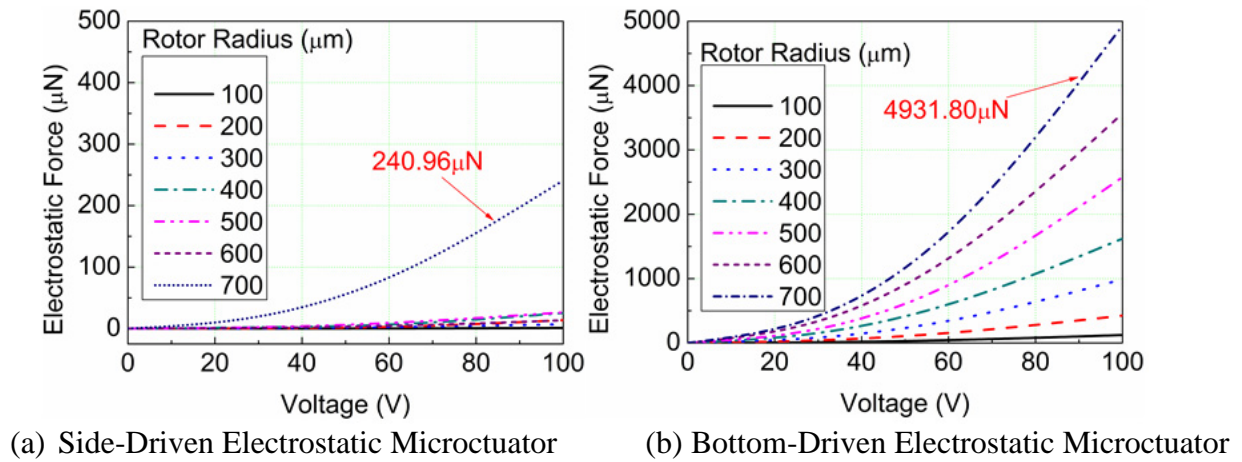


Fig. 3: Comparison of the generated thrust force between the two designs when the size is varied, evaluated with different input voltages.

### Varying Actuator Teeth Ratio

The teeth ratio of both actuators were set to five values; i.e 12:9, 16:12, 20:15, 24:18 and 28:21 respectively, whilst the gap between the stator and the rotor, thickness and size of actuator is fixed to  $2\mu\text{m}$ ,  $50\mu\text{m}$  and  $700\mu\text{m}$ , respectively. Fig. 5 shows the relationship between the teeth ratio of actuator, applied voltage and the generated electrostatic force. From Fig. 5 (a) and (b), the results show that almost all the ratio has the almost similar electrostatic force value. This maybe due to increase number of teeth, thus increasing the overlapping area between stator and rotor electrode. However, simultaneously the distance travel per step input will be decreased. Therefore based on these results, it is concluded that the electrostatic force tends to remain the same when the teeth ratio is increased.

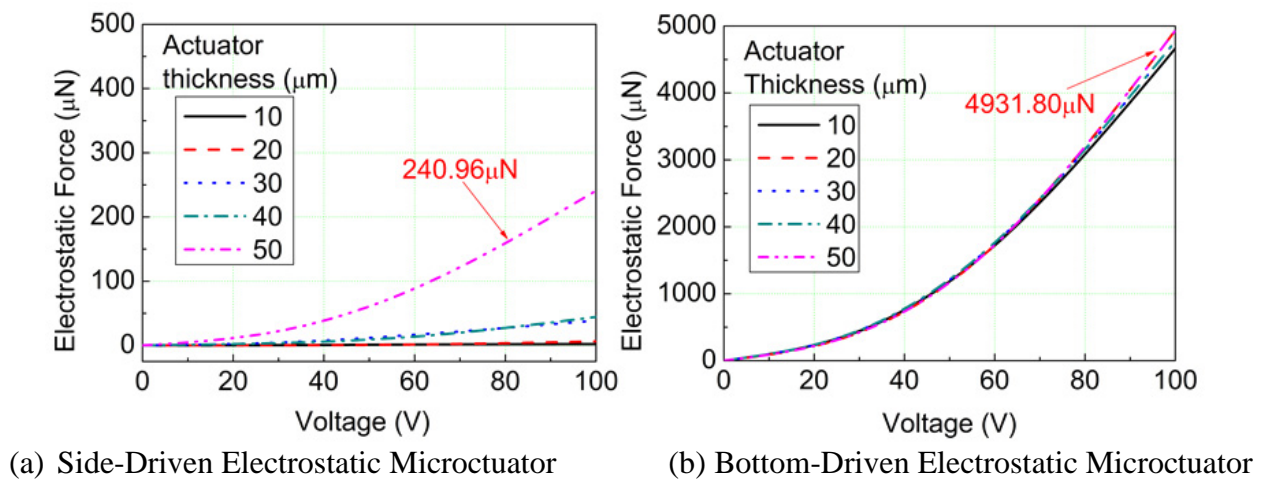
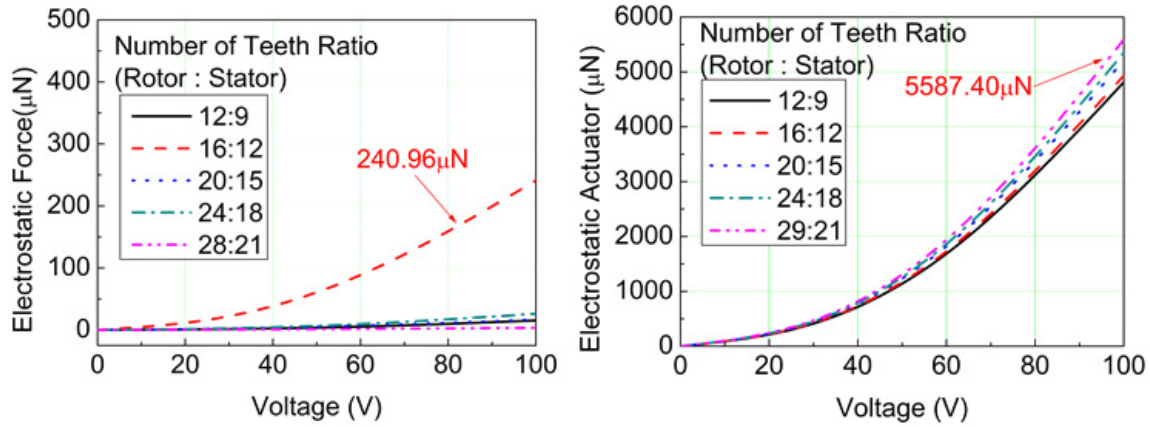


Fig.4: Comparison of the generated thrust force between the two designs when the thickness is varied, evaluated with different input voltages.



(a) Side-Driven Electrostatic Microactuator (b) Bottom-Driven Electrostatic Microactuator

Fig.5: Comparison of the generated thrust force between the two designs when the teeth ratio is varied, evaluated with different input voltages.

## Conclusion

The overall results show that in terms of the generated electrostatic thrust force, the Bottom-Driven microactuator has more advantages compared to the Side-Driven microactuator. Based on the FEM analysis results, both the size and thickness affect the generated electrostatic force of Side-Driven Microactuator significantly, however the thickness does not affect the performances of Bottom-Drive Microactuator. As a conclusion based on Table 3, the FEM analysis results show that the Bottom-Drive Electrostatic Microactuator exhibit greater thrust force, 4931.80 $\mu$ N compared to the Side-Drive Electrostatic Microactuator, 240.96 $\mu$ N; when the actuator's radius is 700 $\mu$ m, thickness is 50 $\mu$ m, gap between the stator and rotor is 2 $\mu$ m and the teeth ratio is 16:12.

Table 3 FEM analysis results of the rotary motion designs

Type	Characteristics	Vary Actuator Size	Vary Actuator Thickness	Vary Actuator Teeth Ratio
Side-Driven	Parameters	700 $\mu$ m	50 $\mu$ m	16:12
	Highest force	240.96 $\mu$ N	240.96 $\mu$ N	240.96 $\mu$ N
Bottom-Driven	Parameters	700 $\mu$ m	50 $\mu$ m	16:12
	Highest force	4931.8 $\mu$ N	4931.8 $\mu$ N	5587.4 $\mu$ N

## Acknowledgement

This research and publication is supported by Universiti Teknikal Malaysia Melaka (UTeM) Short Term Grant no. PJP/2013/FKE(4C)/S01170. Authors are grateful to UTeM for supporting the research.

## References

- [1] M. Karpelson, G.-Y. Wei, and R. J. Wood; "A review of actuation and power electronics options for flapping-wing robotic insects", IEEE International Conference on Robotics and Automation, Pasadena, CA, USA, pp. 779-786 (2008).
- [2] Niino T, Egawa S, Higuchi T.; "Dual excitation multiphase electrostatic drive", Proceeding of the Industry Application Society Annual Meeting. pp.1318-25 (1995).
- [3] E. Sarajlic, C. Yamahata, M. Cordero, L. Jalabert, T. Iizuka, H. Fujita; "Single mask 3-phase electrostatic rotary stepper micromotor", International Conference of Solid-State Sensors, Actuators and Microsystems, pp. 1505 - 1508 (2009).
- [4] N.Ghalichechian, A. Modafe, M. I.Beyaz, R.Ghodssi; "Design, fabrication and characterization of a rotary micromotor supported on microball bearings", Journal of Microelectromechanical Systems, Vol. 17, No. 3, pp. 632 - 642 (2008).